Experimental assessment of static friction between pallet and beams in racking systems

Carlo A. Castiglioni [a], Alberto Drei [a,*], Panayotis Carydis [b], Harris Mouzakis [b]

[a] *Polytechnic University, ABC Department, Milan, Italy*
[b] *National Technical University-Laboratory of Earthquake Engineering, Athens, Greece*

In order to investigate the sliding behavior of pallets stored on steel racking systems, a large number of sliding tests under both static and dynamic conditions were performed within the EU-RFCS Research Project "SEISRACKS: Storage Racks in Seismic Areas". In this paper, the results obtained for the assessment of the Static Friction Factor between pallet and beams are described and commented upon.

Keywords:
Cold formed beam
Pallet
Racking systems
Static friction

1. Introduction

Despite their lightness, racking systems carry very high live load (many times larger than the dead load, opposite of what happens for usual civil engineering structures) and can raise a considerable height.

Racks are widely adopted in warehouses where they are loaded with tons of (more or less) valuable goods. The loss of these goods during an earthquake may represent, for the owner, a very large economic loss, much larger than the cost of the whole rack on which the goods are stored, or of the cost for its seismic upgrade. Racks are also more and more frequently adopted in supermarkets and shopping centers, in areas open to the public. The falling of the pallets, in this case, may endanger the life of the costumers as well as that of the workmen and employees. Sliding of the pallets on the racks and their consequent fall represents a limit state that might occur during a seismic event also in the case of a well designed storage rack, as the phenomenon depends only on the dynamic friction coefficient between the pallet and the steel beams of the rack. Besides the usual global and local collapse mechanisms, an additional limit state for the system is represented by the fall of the pallets with subsequent damage to goods, people and to the structure itself.

* Corresponding author.
E-mail addresses: carlo.castiglioni@polimi.it (C.A. Castiglioni), alberto.drei@polimi.it (A. Drei), pkary@tee.gr (P. Carydis), harrismou@central.ntua.gr (H. Mouzakis).

At present, there are technical limitations in the field of safety and design of storage racks in seismic areas: lack of knowledge on actions challenging the structures, lack of knowledge on structural behavior in terms of ductility and sliding conditions of the pallets on the racks and lack of Standard Design Codes in Europe. To solve some of these limitations, the EU sponsored through the Research Fund for Coal and Steel an RTD project titled "Storage Racks in Seismic Areas" (acronym SEISRACKS, Contract number: RFS-PR-03114), including an experimental research, presented hereafter on static and dynamic friction behavior of the coupling steel beam-wooden pallet, consisting in about 1260 static tests and 182 dynamic tests. This paper is focused only on the results of the static tests, considering the influence of different parameters (such as the type of pallet and beam, the stored mass and the mass eccentricity). Dynamic tests are presented in another paper.

Storage racks are composed of specially designed steel elements that permit easy installation and reconfiguration, consistent with the merchandising needs of a warehouse retail store. Except where adjacent to walls, storage racks normally are configured as two rows of racks that are interconnected. Pallets typically can have plan areas of approximately one square meter and can have a maximum loaded weight of approximately 10–15 kN. Storage rack bays are typically 1.0–1.1 m deep and 1.8–2.7 m wide and can accommodate two or three pallets. The overall height of pallet rack structural frames, found in retail warehouse stores, varies between 5 and 6 m. In industrial warehouse facilities, racking system can reach considerable heights, such as 12–15 m.

Published Journal Article available at: http://dx.doi.org/10.1016/j.jobe.2016.03.004

The rack industry calls the longitudinal direction the down-aisle direction, and the transverse direction the cross-aisle direction. Proprietary moment connections are typically used as the structural system in the down-aisle direction and braced frames are typically used as the structural system in the cross-aisle direction.

2. Friction models

Friction is the tangential reaction force between two surfaces in contact. Physically these reaction forces are the results of many different mechanisms, which depend on contact geometry and typology, properties of the bulk and surface materials of the bodies, displacement and relative velocity of the bodies and presence of lubrication.

In dry sliding contacts between flat surfaces, friction can be modeled as elastic and plastic deformation forces of microscopic asperities in contact. For each asperity contact the tangential deformation is elastic until the applied shear pressure exceeds the shear strength τ_y of the surface materials, when it becomes plastic.

There are different models of friction that consider stationary condition, e.g. constant velocity of the contact surfaces, and other, developed in the last century, that consider friction with a dynamic model.

In the Coulomb [6] model, the main idea is that friction opposes motion and that its magnitude is independent of velocity and contact area (Fig. 2.1a). It can therefore be described as $F=F_C$ $sgn(v)$, where the friction force F_C is proportional to the normal load, i.e. $F_C=\mu F_N$

The Coulomb [6] friction model does not specify the friction force for zero velocity. It may be zero or it can take any value in the interval between $-F_C$ and F_C, depending on how the sign function is defined.

This very simple model is often modified with the introduction of viscosity parameters in order to take into account a dependence on velocity, $F=(F_C+F_V v)sgn(v)$ as shown in Fig. 2.1b.

Stiction (Fig. 2.2a) is short for static friction as opposed to dynamic friction. It describes the friction force at rest. Morin [12] introduced the idea of a friction force at rest that is higher than the Coulomb friction level. Static friction counteracts external forces below a certain level and thus keeps an object from moving. It is hence clear that friction at rest cannot be described as a function of velocity only. Instead it has to be modeled using the external force F_E in the following way: $F=F_E$ if $v=0$ and $|F_E|< F_S$; $F=F_S$ $sgn(F_E)$ if $v=0$ and $|F_E|\geq F_S$.

The friction force for zero velocity is a function of the external force and not of the velocity. The friction force does not decrease discontinuously as in Fig. 2.2a, but the velocity dependence is continuous as shown in Fig. 2.2b. This is called Stribeck friction.

A more general description of friction than the classical models is, therefore: $F=F(v)$ if $v\neq 0$; $F=F_E$ if $v=0$ and $|F_E|< F_S$; otherwise it is $F=F_S\, sgn(F_E)$; where $F(v)$ is an arbitrary function, which can be as in Fig. 2.3.

Function $F(v)$ is easily obtained by measuring the friction force for motions with constant velocity. The curve schematically shown in Fig. 2.2a, is often asymmetrical.

Other static models of friction, as Karnopp model [11] model and Armstrong's [1] model are described by Olsson et al. [13]. Lately there has been a significant interest in dynamic friction models that describe friction as a dynamic system, with differential equations. In the Dahl [7–9] model it is assumed that the friction force is only position dependent, i.e. it depends only on the relative displacement x of the two surfaces. The starting point of this model is the stress–strain curve of the classical solid-mechanics theory. When subjected to stress the friction force increases gradually until rupture occurs. Let x be the displacement, F the friction force and F_c the Coulomb friction force. Then, Dahl's model has the form:

$$\frac{dF}{dx} = \sigma \cdot \left(1 - \frac{F}{F_C}\cdot \mathrm{sgn}(v)\right)^{\alpha}$$

where σ is the stiffness coefficient and α is a parameter that determines the shape of the stress–strain curve. The value $\alpha=1$ is commonly used, while higher values give a stress–strain curve with a sharper bend. Fig. 2.3 shows a graphical representation of this model.

This model is a generalization of the Coulomb model, but it doesn't include the Stribeck effect, which is a rate dependent phenomenon, and does not capture stiction.

Various other dynamic models, generally complex and not described herein, are indicated in bibliography. There are among them that developed by Bliman and Sorine [2–4] based on the experimental investigations of Rabinowicz [14], and another important recent dynamic model, the LuGre Model (Canudas de Wit et al. 1995).

For the assessment of the sliding of pallets on racks, instead of adopting « a priori » one of these models, as it cannot be stated which one fits better the real behavior, it was decided to describe the phenomenon by means of a numerical analysis. Particularly for the sliding of pallets on rack systems, a numerical model was developed within the SEISRACKS project by Denoël and Degée [10], considering a SDOF sliding system subjected to a sinusoidal ground motion $u(t)$ reported in the references.

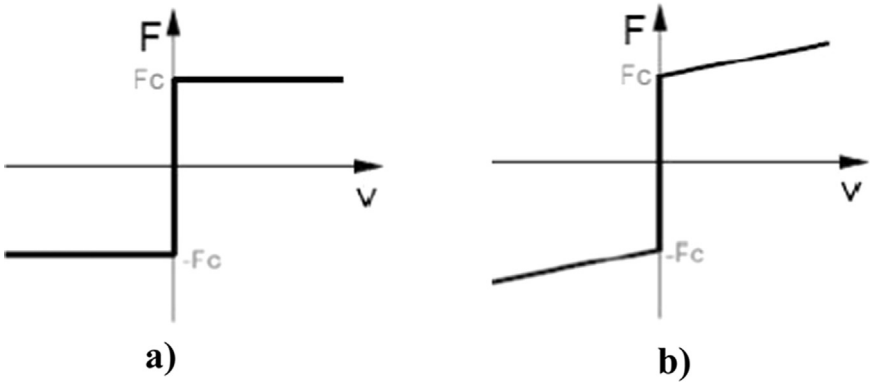

Fig. 2.1. (a) Coulomb friction model, (b) Coulomb friction model with the adding of viscosity.

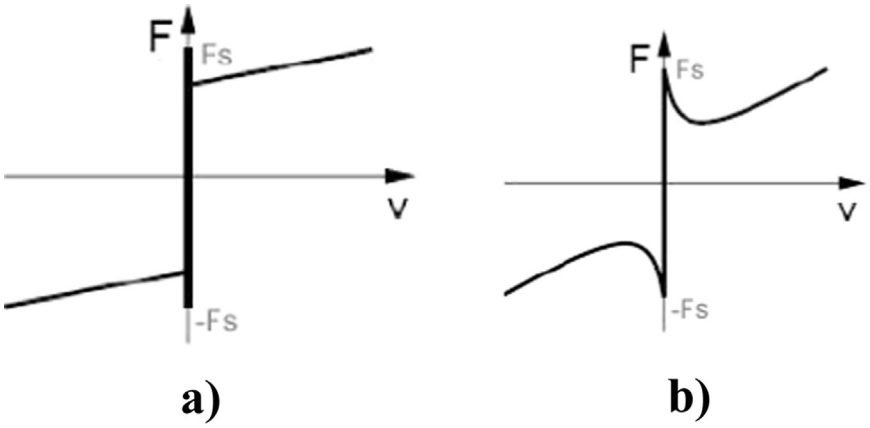

Fig. 2.2. (a) Stiction plus Coulomb model, (b) Coulomb model with continuous decrease of the friction force.

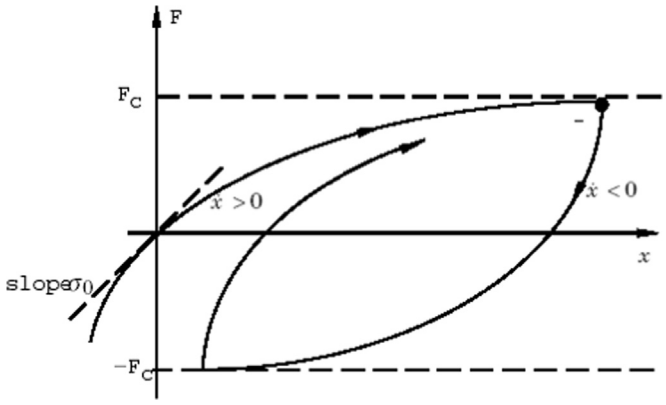

Fig. 2.3. Friction force as a function of displacement for Dahl's model.

3. Assessment of the static friction factor

Quasi static sliding tests were performed at the Laboratory for Earthquake Engineering (LEE) of the National Technical University of Athens (NTUA), Greece. The aim of this group of tests was to obtain the static friction factor for different combinations of beams and pallets, and to study the influence of the mass and of its eccentricity.

The static, as well as the dynamic friction behavior (that has been assessed by means of dynamic tests carried out in the second part of this research) are related to the interaction at the interface between the pallet and the supporting beams.

The test set-up for quasi-static tests is shown in Fig. 3.1. Two horizontal beams are fixed on a rigid steel frame with a pinned support. The frame is free to rotate about the pinned axis. The axial distance between the pinned axis and the free edge of the frame is 1575 mm. One pallet, with a rigidly fixed mass of 8 kN, is positioned on the beams. The system is gradually and slowly inclined with the use of a crane, that lifts the frame from its free edge, while the vertical displacement and the relative displacement between pallet and beam, are measured. In order to minimize any dynamic effect, the vertical displacement of the uplifting points was set less than 10 mm per second. Moreover, the difference in uplifting of the two sides of the support was checked, and with a maximum accepted difference of 4 mm.

Thirty repetitions of each test (combination of pallet and beam) are carried out. These tests were performed in down and cross-aisle direction.

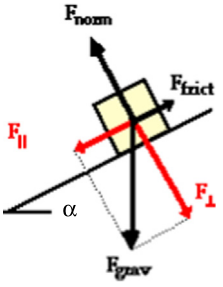

$$F_{II} = F_{grav} \cdot \sin(\alpha) = F_{frict} = \mu \cdot F_{grav} \cdot \cos(\alpha)$$

hence :

$$\mu = \tan(\alpha)$$

Fig. 3.2. Principle of inclined plane.

Fig. 3.1. Experimental set-up for quasi-static sliding tests.

a) b) c)

Fig. 3.3. Different types of pallet: (a) Wooden Euro pallet, (b) Wooden American, (c) Plastic Euro pallet.

Fig. 3.4. examples of beam sections: type B1, type B4 and type B6.

Static tests are based on the principle of the inclined plane shown in Fig. 3.2, in which, when the pallet starts to slide, the component of the gravity force along the beam (F_{II}) is equal to its perpendicular component ($F_{\perp}$) multiplied by a static friction factor μ.

Different types of pallets and beams were used during the experimental tests as shown respectively in Figs. 3.3 and 3.4. With pallet type P1 three different values of the applied mass were considered (251 kg, 785 kg, 1036 kg) as well as the different position of the mass on the pallet (centered, eccentric downward, eccentric upward) (Table 3.1).

Seven types of pallets and six types of beam were used in the tests, with the following denomination:

Pallet P1 is a wooden Euro pallet, new and dry. Usually, after being in use for a while, the lower faces of the pallet wear out. For this reason the normal situation is that represented by pallet P2, a wooden Euro pallet old and dry. In order to investigate eventual environmental conditions, pallet P3 is an old wooden Euro pallet, that was spread with water for a few minutes, before testing.

The same conditions were considered also for the American type of pallets, respectively P4, P5, and P6.

Table 3.1
Type of pallet and beam used in the different tests.

Pallets	Beams
P1: Wooden Euro pallet 800 × 1200, new, dry	B1: Cold rolled, powder coated, new (Producer A)
P2: Wooden Euro pallet 800 × 1200, old, dry	B2: Cold rolled, hot dip coated, new (Producer A)
P3: Wooden Euro pallet 800 × 1200, old, wet	B3: Cold rolled, hot zinc coated, new (Producer A)
P4: Wooden American pallet, new, dry	B4: Cold rolled, hot dip coated, new (Producer B)
P5: Wooden American pallet, old, dry	B5: Cold rolled, hot dip coated, new (Producer C)
P6: Wooden American pallet, old, wet	B6: Cold rolled, hot dip coated, new (Producer C)
P7: Plastic Euro pallet	

Pallet P7 is a plastic Euro pallet. This type of pallet is more and more adopted, as it is more resistant and can be more easily cleaned than the wooden one. It is widely adopted, for example, for the storage of food, in particular in refrigeration units.

Six different types of beams, manufactured by three different companies were considered. Beams B1, B2 and B3 were manufactured by the same company (A): the cross section was the same for all the three types, but surface treatment was different. B1 was powder coated beam, B2 was a hot dip coated beam and B3 a hot zinc coated beam.

Beam B4 was manufactured by a different company (B), with a different cross section than the previous ones, and a powder coating surface treatment.

Beam B5 and B6 were manufactured by another company (C) and differ for their geometry, although surface treatment was the same type of powder coating for both beams.

4. Static friction in cross-aisle direction

Sliding in this direction is very dangerous because the pallet width is 1200 mm while the rack width is usually 1100 mm. Hence, a few mm of displacement, eventually correlated to a small eccentricity of positioning, can result in a loss of support of the pallet.

Table 4.1
Symbols used in the statistical analysis of the data.

μ	Mean value	
σ	Standard deviation	
Cov %	Coefficient Of Variation %	$Cov\,\% = \frac{\sigma}{\mu}\cdot 100$
Max	Maximum value	
Min	Minimum value	
Δ^+ %	Difference percentage between the maximum value and the mean one	$\Delta^+\% = \frac{Max-\mu}{\mu}\cdot 100$
Δ^- %	Difference percentage between the minimum value and the mean one	$\Delta^-\% = \frac{\mu-Min}{\mu}\cdot 100$
α^+	Difference between the maximum value and the mean one in terms of standard deviation	$\alpha^+ = \frac{Max-\mu}{\sigma}$
α^-	Difference between the mean value and the minimum one in terms of standard deviation	$\alpha^- = \frac{\mu-Min}{\sigma}$

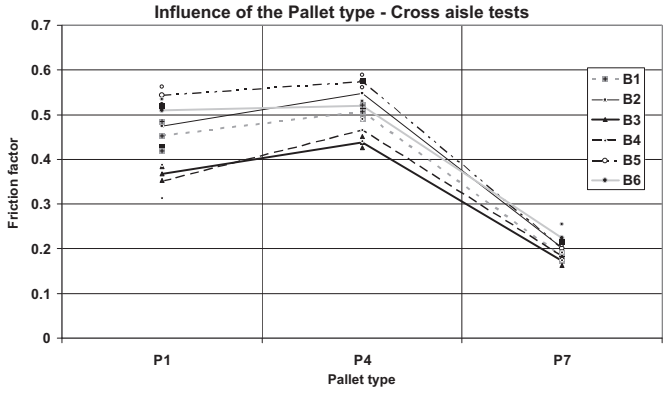

Fig. 4.1. Influence of the pallet type on the friction factor in cross-aisle direction, for different types of beam.

In the next paragraphs for the new pallets, type P1, P4 and P7, all the figures show the mean values of the static friction factor, with the indication of the standard deviation, for every test type. All the tests are repeated 30 times in the same conditions, and the final table reports a statistical analysis of the experimental results. In the following, reference will be made to the statistical parameters described in Table 4.1. The data for old wood pallets, type P2, P3, P5 and P6, corresponding to the new pallets P1 and P4, are not reported in the following, as the results obtained are practically the same of the new types. Even wet conditioning of pallet had no effect. Representing only pallets P1, P4 and P7, the differences among Euro pallet, American pallet and Plastic Euro pallet are better enlightened.

4.1. Influence of the pallet type

Fig. 4.1 shows the influence of the pallet type on the static friction factor in cross-aisle direction, while Table 4.2 presents the statistics of the results. All the tests are carried out with a mass of 785 kg centered on the pallet.

It can be observed that:

- Pallet P4 (American Wooden Pallet) has the highest mean value of the friction factor (0.51), while pallet P7 (Plastic Euro Pallet) has the lowest. Pallet P1 (Wooden Euro Pallet) has an intermediate value, very close to that measured for Pallet P4.
- Scatter of the data for all pallets is limited, with c.o.v. ranging from 9.8% (P4) to 16.9% (P1), in particular P4 has the lowest scatter of the data, P1 has the highest one and P7 has an intermediate value.

4.2. Influence of the beam type

Similar considerations can be drawn with regards to Fig. 4.2 that shows the influence of the beam type. Tests are carried out with a centered mass of 785 kg. Test results and their statistical reanalysis, for Pallets P4 and P7, are presented in Table 4.3 and 4.4

It can be observed that:

- Pallet P4 (American wooden Pallet) shows the highest value of the friction factor, pallet P1 (Wooden Euro Pallet) an intermediate one and pallet P7 (Plastic Euro Pallet) the lowest one.
- Friction factor for pallet P7 is quite constant, while for the other two types of pallet the friction factor shows a strong dependence on the beam type. In particular the lowest values are obtained for beam types B3 and B4, while in the other cases the friction factor is similar.
- For pallets P1 and P4 the highest friction factor is obtained with beam B5.
- The behavior of the American wooden pallet and the wooden Euro pallet is very similar.

The following tables present the re-analysis of the results in case of pallet P1 and P4 (Wooden Euro pallet and American pallet) and of the groups of beams B1+B2+B5+B6 (Table 4.5), B3 (Table 4.6) and B4 (Table 4.7).

Table 4.2
Statistics of test results for different types of pallet.

	μ	σ	*Cov%*	*Max*	*Min*	Δ^+ %	Δ^- %	$\mu+\sigma$	$\mu-\sigma$	$\mu+2\sigma$	$\mu-2\sigma$	α^+	α^-
P1	0.45	0.08	16.9	0.58	0.27	28.7	39.7	0.53	0.37	0.60	0.30	1.70	2.35
P4	0.51	0.05	9.8	0.61	0.41	19.5	18.5	0.56	0.46	0.61	0.41	2.00	1.89
P7	0.19	0.02	11.8	0.34	0.16	72.9	19.6	0.22	0.17	0.24	0.15	6.18	1.66

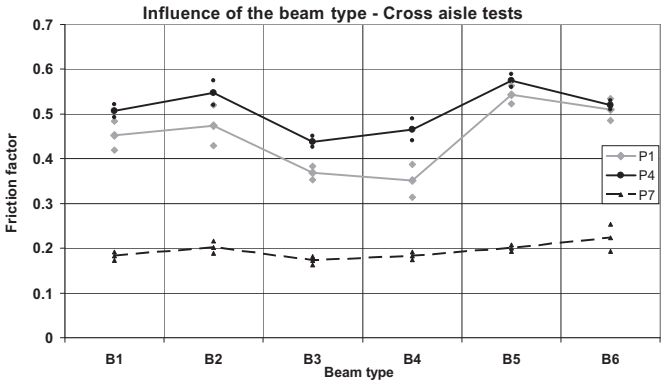

Fig. 4.2. Influence of the beam type on the friction factor in cross-aisle direction, for different types of pallet.

It can be noticed that the response of the groups of beams (B1+B2+B5+B6) is rather homogeneous. A mean value of the static friction factor of 0.52 was obtained, with a c.o.v. of 8.9%.

In the case of the beam types B3 and B4, data seem to be less homogeneous than those of the other group of beams. Mean values of the static friction factor respectively 0.40 and 0.41, with a c.o.v. of 13.1% and of 15.8%, were obtained.

It is evident that the static friction factor developed by the first group of beams is much higher than the one developed by the beam types B3 and B4.

The following Fig. 4.3 shows the repetition of tests for pallet type P1 and beams B1. The observed behavior for other types of beams (B2, B3, B4, B5, B6) is similar, therefore the reported graph is quite exemplary, also for other types of pallets.

It can be noticed that, in the first tests, the friction factor shows an increasing trend while, after 5–10 tests, the obtained value is practically constant. This is most probably due to the "wearing" of the surface of the beam. In the first tests, the beam is new, and the friction factor is low. Due to wearing, the surface roughness increases, together with the friction factor as well as the scatter of the results. Beyond a certain level, the phenomenon stabilizes.

4.3. Influence of the applied mass

Fig. 4.4 shows two of the three masses used in the tests. The influence of the applied mass is measured with masses of 251 kg, 785 kg and 1036 kg, for pallet type P1 and for different types of beam. The mass is fixed on the pallet so that there is no relative displacement.

Fig. 4.5 shows the influence of the beam type on the friction factor in cross-aisle direction, for different values of the applied masses.

Table 4.3
Statistics of test results for Pallet P4 and different types of beam.

	μ	σ	*Cov%*	*Max*	*Min*	Δ^+ %	Δ^- %	$\mu+\sigma$	$\mu-\sigma$	$\mu+2\sigma$	$\mu-2\sigma$	α^+	α^-
B1	0.51	0.01	2.9	0.53	0.46	5.2	9.1	0.52	0.49	0.54	0.48	1.80	3.13
B2	0.55	0.03	5.1	0.59	0.47	8.3	13.3	0.58	0.52	0.60	0.49	1.63	2.62
B3	0.44	0.01	2.7	0.46	0.41	5.4	5.5	0.45	0.43	0.46	0.42	2.00	2.05
B4	0.47	0.02	5.2	0.51	0.42	9.2	9.1	0.49	0.44	0.51	0.42	1.77	1.73
B5	0.57	0.01	2.5	0.61	0.54	5.7	5.3	0.59	0.56	0.60	0.55	2.33	2.13
B6	0.52	0.01	2.0	0.54	0.49	3.3	5.0	0.53	0.51	0.54	0.50	1.65	2.45

Table 4.4
Statistics of test results for Pallet P7 and different types of beam.

	μ	σ	*Cov%*	*Max*	*Min*	Δ^+ %	Δ^- %	$\mu+\sigma$	$\mu-\sigma$	$\mu+2\sigma$	$\mu-2\sigma$	α^+	α^-
B1	0.18	0.01	5.2	0.20	0.16	11.7	11.0	0.19	0.17	0.20	0.16	2.24	2.10
B2	0.20	0.01	6.8	0.25	0.18	24.0	12.5	0.22	0.19	0.23	0.17	3.51	1.83
B3	0.17	0.01	5.7	0.19	0.16	10.5	9.3	0.18	0.16	0.19	0.15	1.85	1.63
B4	0.18	0.01	4.6	0.21	0.17	14.8	5.9	0.19	0.17	0.20	0.17	3.25	1.30
B5	0.20	0.01	3.6	0.22	0.19	11.7	4.6	0.21	0.19	0.22	0.19	3.22	1.27
B6	0.22	0.02	8.5	0.26	0.19	20.6	11.2	0.24	0.20	0.25	0.18	2.42	1.32

Table 4.5
Statistics of test results considering Pallet P1+P4 and beams B1+B2+B5+B6.

	μ	σ	*Cov%*	*Max*	*Min*	Δ^+ %	Δ^- %	$\mu+\sigma$	$\mu-\sigma$	$\mu+2\sigma$	$\mu-2\sigma$	α^+	α^-
B1+B2 B5+B6	0.52	0.05	8.9	0.61	0.37	17.8	28.5	0.56	0.47	0.61	0.42	2.01	3.21

Table 4.6
Statistics of test results considering Pallet P1+P4 and beam B3.

	μ	σ	*Cov%*	*Max*	*Min*	Δ^+ %	Δ^- %	$\mu+\sigma$	$\mu-\sigma$	$\mu+2\sigma$	$\mu-2\sigma$	α^+	α^-
B3	0.40	0.04	9.4	0.46	0.33	14.6	18.0	0.44	0.37	0.48	0.33	1.56	1.92

Table 4.7
Statistics of test results considering Pallet P1 + P4 and beam B4.

	μ	σ	Cov%	Max	Min	Δ^+ %	Δ^- %	$\mu+\sigma$	$\mu-\sigma$	$\mu+2\sigma$	$\mu-2\sigma$	α^+	α^-
B4	0.41	0.06	15.8	0.51	0.27	24.3	33.8	0.47	0.34	0.54	0.28	1.53	2.14

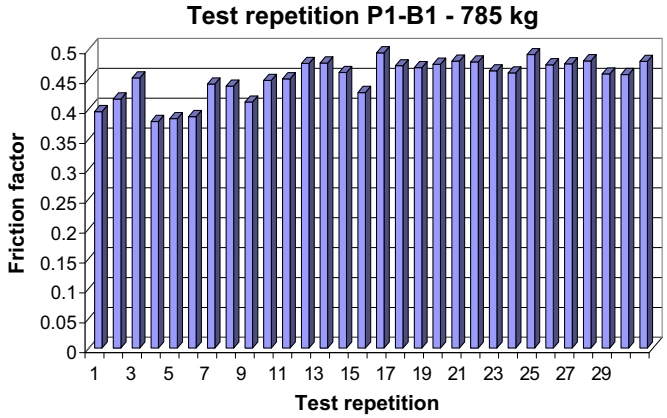

Fig. 4.3. Repetition of tests carried out with pallet type P1-beam type B1.

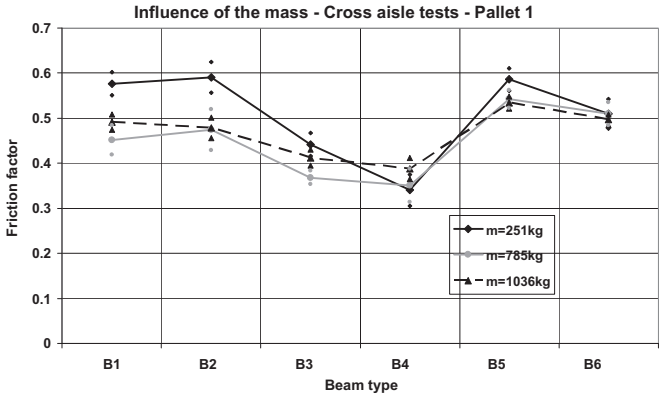

Fig. 4.5. Friction factor in cross-aisle direction – influence of the beam type for different applied masses.

Fig. 4.6 shows the influence of the mass, for different types of beam. It can be observed that:

- Applied mass strongly influences the friction factor only for beams B1, B2 and B3, while in the other cases it is quite constant. In every case the standard deviation of all the data is rather limited, with a c.o.v. ranging from 11.5% to 19.4%. It can be noticed that the scatter of the data decreases when the applied mass increases.
- Usually, the highest value of the friction factor is obtained with the mass of 251 kg independently of the beam type, while the lowest one with the intermediate mass. Exceptions are beams B4 and B6.

As expected, the value of the applied mass influences the response of the system less than the other analyzed parameters.

The mean values of the static friction factor are practically non influenced by the value of the applied mass.

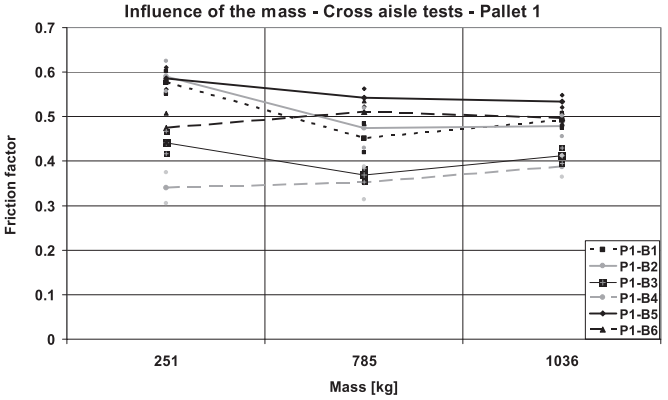

Fig. 4.6. Influence of the applied mass on the friction factor in cross-aisle direction, for different type of beam.

Fig. 4.4. Different types of the applied mass: (a) 251 Kg (b) 785 Kg.

5. Static friction in down-aisle direction

In practice, sliding in this direction is less dangerous than in cross-aisle direction, because fall of the pallet can occur only if a rotation around the vertical axes is associated with the pallet displacement. In any case, with the test set up shown in Fig. 5.1, quasi-static sliding tests were carried out analyzing the same parameters as in the tests in cross-aisle direction, in order to allow a comparison between static friction factor values in the two directions.

Fig. 5.1. Set up for down-aisle tests.

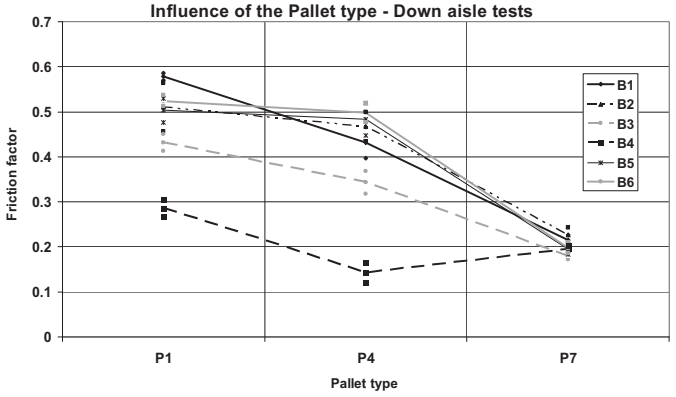

Fig. 5.2. Influence of the pallet type on the friction factor in down-aisle direction, for different types of beam.

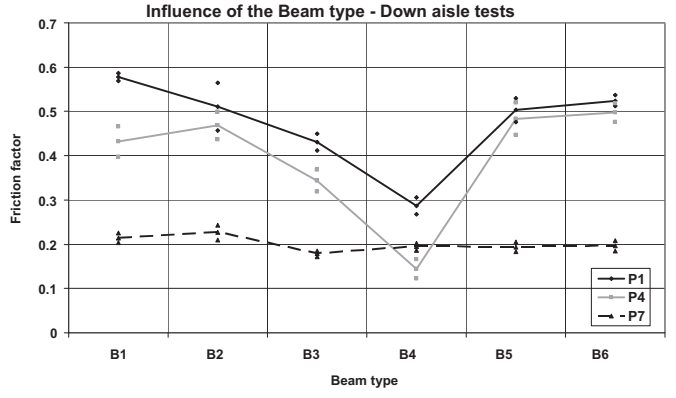

Fig. 5.3. Influence of the beam type on the friction factor in down-aisle direction, for different types of pallet.

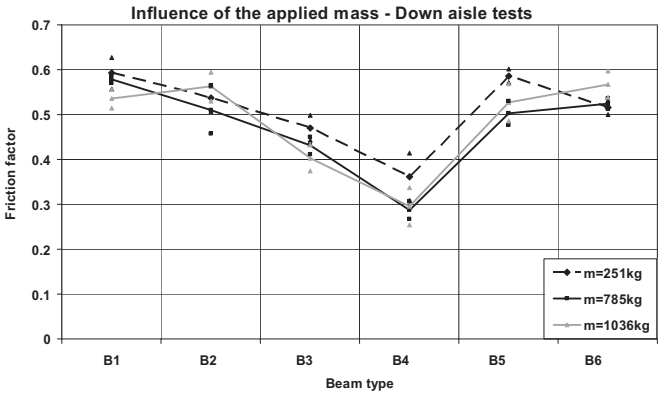

Fig. 5.4. Down-aisle direction – influence of the beam type for different values of the applied masses.

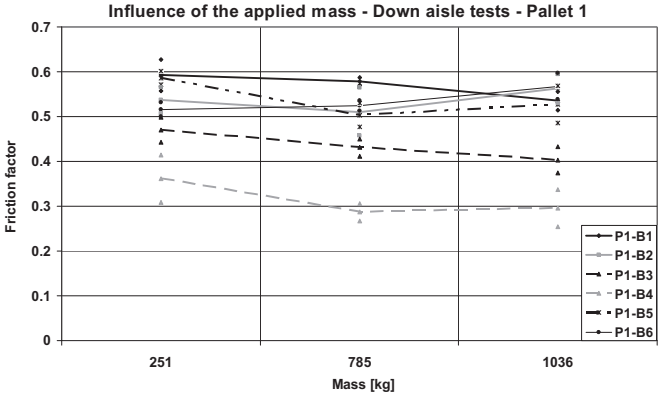

Fig. 5.5. Influence of the applied mass on the friction factor in down-aisle direction, for different types of beam.

5.1. Influence of the pallet type

Fig. 5.2 shows the influence of the pallet type on the friction factor in down-aisle direction, for different types of beam.

5.2. Influence of the beam type

Similar results can be obtained showing the influence of the beam type on the friction factor, for a mass of 785 kg centered on the pallet, as evidenced in Fig. 5.3.

- Friction factor is generally higher for pallet P1 (wooden Euro pallet). Pallet P7 (plastic Euro pallet) shows the lowest friction factor. Pallet P4 (wooden American pallet) has an intermediate behavior.
- Plastic pallet (P7) shows practically the same friction factor independently on the beam type.
- Behavior of the friction factor for pallet P1 and P4 is quite similar: the lowest value is obtained for beam type B4; beam types B1, B2, B5 and B6 have more or less the same value.
- Scatter of the results is very large with a c.o.v. ranging from 29.6% to 37.0%.
- It's important to observe, by comparison of Fig. 5.3 and 4.2, that the friction factors, in cross aisle and down-aisle directions, have values of the same order, apart when wood pallets interact with beam type B4. Particularly, for the American pallet P4 the friction factor in down-aisle reduces to about one third of the cross-aisle value, while for the Euro pallet P1 the reduction is about 20%.

Nevertheless, American pallet P4 shows generally a better behavior with respect to Euro pallet in cross-aisle direction (Fig. 4.2).

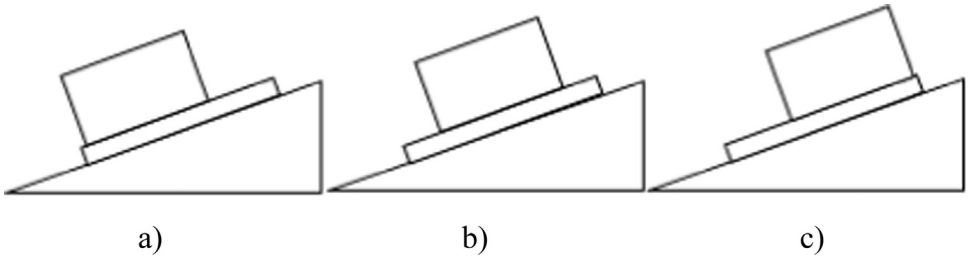

Fig. 5.6. Mass eccentricity: (a) eccentric downward (b) centered (c) eccentric upward.

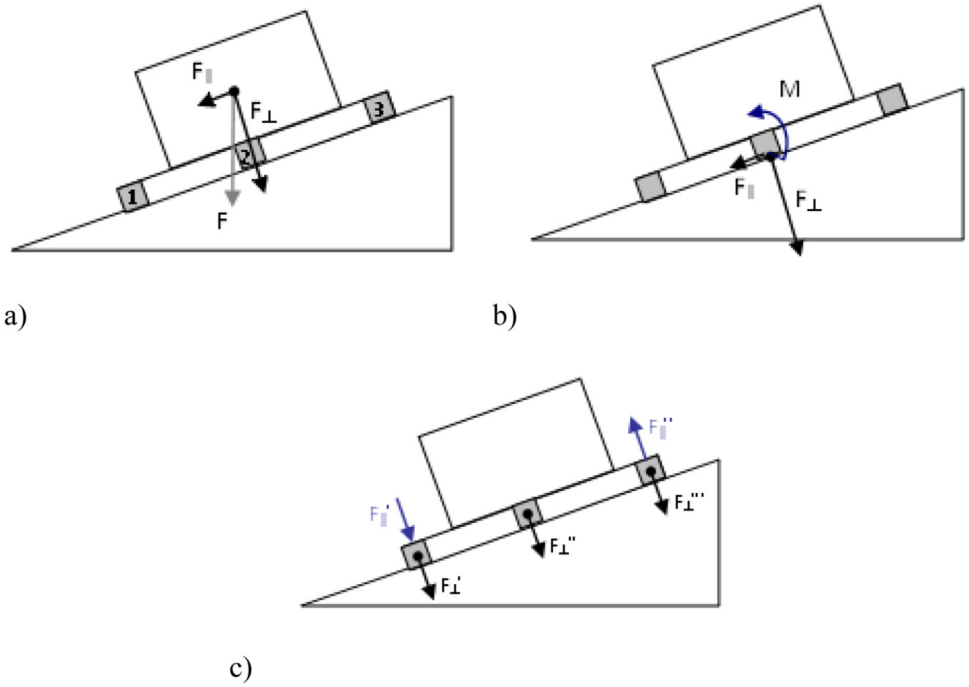

Fig. 5.7. Different component of the forces on the mass during the test.

This non adequate down-aisle behavior can be attributed mainly to the surface treatment of the beam.

5.3. Influence of the applied mass

The influence of the mass is measured on the same pallet type P1 (Wooden Euro pallet) positioning the mass on the pallet without eccentricity and considering different types of beams.

Fig. 5.4 shows the influence of the beam type on the friction factor in down-aisle direction for different values of the applied mass.

The same consideration drawn in case of cross-aisle direction holds: the mass does not influence the static friction factor in down-aisle direction.

Finally, it can be concluded that the variation of the mass has a limited influence on the value of the friction factor. In any case, such an influence is lower than the one of other parameters like pallet and beam types.

The different masses applied (Fig. 4.4), imply a different height of the center of gravity, and therefore an additional forward displacement of the c. o. g. (of the order of 5–10 cm) during the test, due to the uplifting of one side of the steel base frame.

This forward displacement has a negligible effect. It can be seen also from comparison between Fig. 5.3, where is reported the friction factor for the couple pallet P4 – beam B6, and the effect of a forward eccentricity for the same couple in Fig. 5.9: no sig-nificant change in the friction factor happens (0.49 forward ec-centric mass, 0.50 centered mass). A specific analysis of the effect of mass eccentricity is reported in the following. Fig. 5.5

5.4. Influence of the mass eccentricity

The influence of the mass eccentricity was investigated only in the down-aisle direction. The position of the mass on the pallet determines a different distribution of the weight force on the beam, that can influences the value of the friction factor.

Fig. 5.6 shows the position of the mass in the three analyzed cases.

The weight of the mass can be divided in two components, $F_{\perp}$and $F_{\parallel}$ due to the inclined plane. The former component decreases during the test performed increasing the inclination θ of the plane on the horizontal, the latter increases, being:

$$F_{\perp} = F \cdot \cos(\vartheta)$$
$$F_{\amalg} = F \cdot \sin(\vartheta)$$

The orthogonal component $F_{\perp}$can be considered distributed on the three series of blocks of the pallet with the three components $F_{\perp}', F_{\perp}''$ and $F_{\perp}'''$(as shown in Fig. 5.7.c). The parallel component $F_{\parallel}$ (applied in the c.o.g. of the mass) is resisted by the "friction", on the beam-to-pallet interface. As a consequence $F_{\parallel}$ has a lever arm with respect to the sliding plane, where the friction reaction develops. Hence, the effect of $F_{\parallel}$ can be represented as shown in Fig. 5.7.b, where M is the transport moment of $F_{\parallel}$ that has been "moved" from the c.o.g. to the beam-to-pallet interface. Effect of

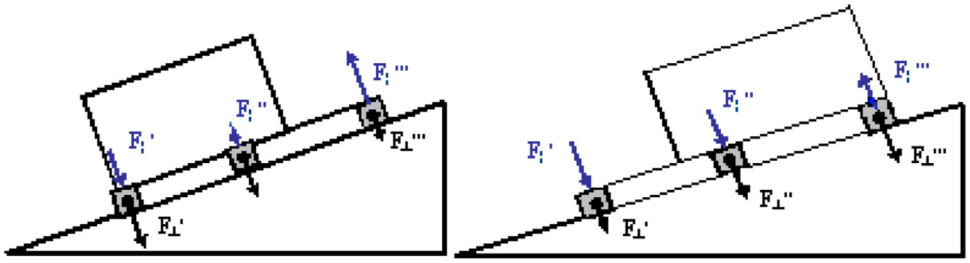

Fig. 5.8. Components of the forces in a downward (a) and upward (b) position.

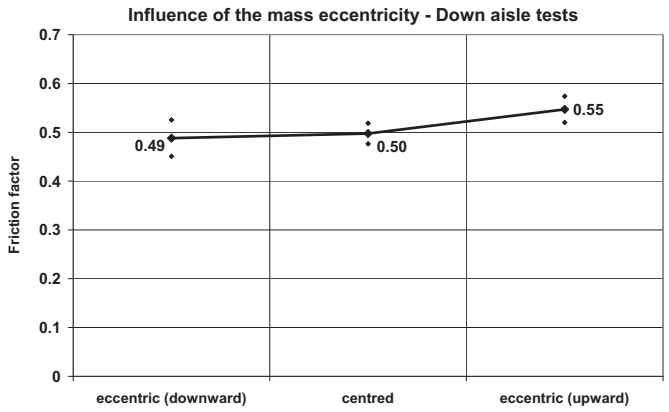

Fig. 5.9. Influence of the mass eccentricity on the friction factor in down-aisle direction.

such a moment (an overturning moment) is to increase the reaction on the wooden block no. 1 with the force $F_{\parallel}'$, and to decrease the one on the third block with the $F_{\parallel}''$ component, as shown in Fig. 5.6.c.

When the mass is positioned downward the orthogonal reaction on the block no. 3 is lower than that on blocks no. 1 and 2. Furthermore, the effect of the overturning moment is to increase the reaction on block no. 1 and reduce that on block no. 3. The result is an "uplift" of the block no. 3, i.e. a reduction of the contact surface (Fig. 5.8.a).

If the mass is centered on the pallet this effect is reduced. On the contrary, when the mass is positioned with an "upward" eccentricity, the effect due to the overturning moment somehow compensates the non-uniform distribution of the reactions perpendicular to the sliding surface resulting in a more uniform distribution of the weight of the pallet, "maximizing" the contact surface (Fig. 5.8.b).

Fig. 5.9 shows the results of the tests, carried out with the combination of Pallet type P4 (Wooden American Pallet) with a beam type B6.

Experimental results confirm the previous considerations. When the mass is positioned with an upward eccentricity, the measured friction factor is larger than in the case with the downward eccentricity. The centered mass develops a friction factor larger than in the case of downward eccentricity.

The variations of the friction coefficient due to differences in the eccentricity of the mass are in any case very small. The slightly increasing trend of the parameter can be explained with the force distribution as shown before. Passing from the downward to the upward position of the mass, the reaction forces on the beam-pallet interface are more balanced, the contact area is maximized and the friction factor increases.

Although this trend has been investigated only for one combination of beam and pallet, the feeling is that this conclusion can be generalized.

6. Dynamic testing and normative perspectives

In the EU-RFCS project SEISRACKS 1, also dynamic tests, to be published in another paper, were performed. The results obtained both from static and Dynamic testing have been used as background of the new EN-16681 code for Seismic Design od Steel Storage Pallet Racking System recently published by CEN. Now, after the official release of EN-16681, the authors felt free to release the experimental results and to make the international scientific community apart of their value. The authors refer to EN-16681 code for the values and the procedure to be adopted in practical design applications.

A large reference on pallet-rack system behavior can be found in [5] "Seismic Behavior of Steel Storage Pallet Racking System" – Research for Development Series, Springer-Verlag, ISBN 978-3-319-28465-1.

In what regards the use of different kind of pallets and beams, for the assessment of the static friction coefficient, also a standard testing procedure was proposed. The friction coefficient to be adopted from experimental activities was set to its characteristic value.

A few words can be added about the results of the 182 dynamic tests performed on the shaking table facility of the Laboratory of Earthquake Engineering (LEE) of the National Technical University of Athens (NTUA), on groups of three pallets, the typical load of a bay of the rack.

Different types of "sliding" test were performed, considering different combinations of beams (type B1, B2 and B3) and Wooden Euro Pallet 800×1200 mm old and dry, both in cross-aisle and down-aisle direction. Most tests were carried out with a sinusoidal excitation, with constant frequency, from 1.0 Hz to 4.0 Hz, and increasing acceleration, mainly in cross-aisle direction. A group of 27 sinusoidal tests with constant amplitude of the acceleration and increasing frequency (displacement amplitude decreases) was performed in down-aisle direction, finally 22 tests were carried out with a seismic shake from three recorded motions of Greek earthquakes, appropriately scaled.

Due to the lateral deformability of the beam in cross-aisle direction, there is a high amplification of the accelerations of masses and beams with respect to that of the shaking table. The acceleration of the beam has a continuously increasing trend while the

acceleration of the mass increases up to a certain level and then remains constant while sliding occurs.

In these tests were determined two main parameters: a "lower bound" and an "upper bound" of the acceleration. Beyond the lower bound acceleration pallets start sliding on the steel beams. When the acceleration of the mass is lower than such "lower bound", the pallet "sticks" on the beams, and no sliding occurs. When the "lower bound" of acceleration is exceeded, increasing the acceleration of the input motion results in a lower increment in the mass acceleration, until an "upper bound" of the mass acceleration is reached. Any further increase in the acceleration of the input motion doesn't affect the acceleration of the mass that is "free" to slide on the beams. "Stiction" between pallet and beam is not resumed until a reduction of the acceleration occurs.

The second parameter is the maximum value of the acceleration of the pallet, during sliding. Hence, this value is associated to the maximum force eventually acting on the structure during a dynamic event: beyond this value, pallets are sliding and their mass can be considered independent of the structure. Higher acceleration values affect only the structural masses that are just a small percentage of the masses stored on the pallets. The upper bound of the sliding acceleration can be obtained only by the reanalysis of those tests in which its trend becomes constant.

A peculiar aspect of the sliding phenomenon observed in some test, is a difference of phase among the shaking table, the beam and the masses after the beginning of sliding. At the end of the test the sliding of the pallet on the beam is evident: in some cases, the pallet was nearly losing the support.

In some tests, especially those carried out at low frequency, sliding did not occur or was limited, and in most cases the acceleration didn't reach an upper bound value. The tests, in fact, had to be stopped when the maximum horizontal excursion of the shaking table reached ± 100 mm. For low frequency (e.g. 1.0 Hz) this condition occurred for acceleration of the shaking table of approximately 0.2 g, a value lower than the upper bound of the sliding acceleration.

In many cases, no sliding of the central pallet was observed in low frequency tests.

Dynamic behavior in cross-aisle direction is completely different to the one in down-aisle direction.

In cross-aisle direction, the flexural stiffness of the beams in the horizontal plane as well as their torsional stiffness influence very much the results. In particular, such stiffnesses are affected by the out-of-plane and torsional behavior of the beam-to-upright connections, whose stiffness rapidly deteriorates under cycling. Test results show, in general, a dependence of the sliding acceleration on the frequency of the input motion. Both the lower and the upper bound of the sliding acceleration seem to decrease when increasing the frequency of the excitation. Lower bound sliding acceleration as low as 0.1 g was measured, for wooden pallets on hot dip coated steel beams. Upper bound values of the acceleration ranging from 0.3 g to 0.5 g were measured depending on the type of beam surface finish as well as on the position of the pallet (laterals or central one).

In down-aisle direction, the sliding acceleration is in general higher than the one measured in cross-aisle direction, under the same testing conditions, with a lower bound of the measured sliding acceleration of nearly 0.3 g, and an upper bound of nearly 0.6 g. Also in down-aisle direction, test results show, in general, a dependence of the sliding acceleration on the frequency of the input motion. However, in this case, both the lower and the upper bound of the sliding acceleration seem to increase when increasing the frequency of the excitation.

Results of tests carried out with constant acceleration and increasing frequency are fully compatible with those obtained in tests with constant frequency and increasing acceleration.

The results obtained with seismic tests, compared with those of tests carried out with a sinusoidal excitation, show full compatibility. Measured sliding accelerations range from 0.15 g to 0.35 g in cross-aisle direction and from 0.45 g to 0.6 g in the down-aisle direction. Similar compatibility was also obtained for bi-directional seismic tests, when comparing the resultants of the vector-compositions of the components of the sliding accelerations in the two orthogonal directions.

7. Conclusions

Assessment of the static sliding conditions of pallets stored on steel racking systems was carried out within the EU- RFCS SEISRACKS 1 research project, by means of static tests performed at the Earthquake Engineering Laboratory of the National Technical University of Athens.

Static tests were carried out in both down and cross-aisle direction, by means of an "inclined plane" device, by slowly increasing the inclination of the plane, and measuring the sliding of the pallet on the rack steel beams.

Influence of the following parameters was investigated:

Type of beam (namely type of surface finish of the beam)

Type of pallet (namely geometry and wear conditions)

Geometry and weight of mass resting on the pallet

Influence of the type of beam was investigated by adopting six different types of beam specimens, manufactured by three different producers, with different types of surface finish. In particular, hot zinc, hot dip and powder coated steel beams were considered.

In both cross and down-aisle direction, the surface finish influenced very much the static friction factor, with differences as large as 20–30% from one type to the other, in the case of wooden pallets.

Influence of the type of pallet was investigated by adopting three different types of pallets, namely: wooden Euro pallets, wooden American-pallet and plastic Euro pallet. In both cross and down-aisle direction the plastic Euro pallet showed a very low friction factor (of the order of 0.2), practically being non-influenced by the type of beam surface finish. The wooden pallets show a very similar friction factor (of the order of 0.5), and are similarly influenced by the beam surface finish. In both cross and down-aisle direction, the mass weight did not affect much the results. However, its geometry (height of the c.o.g.) and its "placement" on the pallet (centered or eccentric) resulted in small variations of the measured friction factor.

References

[1] B. Armstrong, P. Dupont, C. Canudas de Wit, A survey of models, analysis tools and compensation methods for the control of machines with friction, Automatica 30 (7) (1994) 1083–1138.

[2] Bliman P.A., Sorine M., 1991. Friction modelling by hysteresis operators. application to Dahl, sticktion and Stribeck effects. In: Proceedings of the Conference "Models of Hysteresis", Trento, Italy.

[3] Bliman P.A., Sorine M., 1993. A system-theoretic approach of systems with hysteresis. Application to friction modelling and compensation. In: Proceedings of the second European Control Conference, Groningen, The Netherlands, pp. 1844–1849.

[4] Bliman P.A., Sorine M., 1995. Easy-to-use realistic dry friction models for automatic control. In: Proceedings of the 3rd European. Control Conference, ECC'95, Rome, Italy, pp. 3788–3794.

[5] C.A. Castiglioni, Seismic Behaviour of Steel Storage Pallet Racking System Research for Development Series, Springer-Verlag, 2016, ISBN 978-3-319-28465-1.

[6] C.A. Coulomb, Essai sur une Application des Regles de Maximis et Minimis à Quelques Problemes Relatifs à l'architecture, Memoires de Mathèmatique et de Physique,, Academie Royale des Sciences, Paris 1776, pp. 343–382.

[7] Dahl, P.R., 1968. A Solid Friction Model, The Aerospace Corporation, El Segundo CA, Tech. Rep. TOR- 0158 3107 3118.

[8] Dahl P.R., 1975. Solid friction damping of spacecraft oscillations, AIAA Paper

no.75-1104, AIAA Guidance and Control Conference, Boston, USA.
[9] P.R. Dahl, Solid friction damping of mechanical vibrations, AIAA J. 14 (12) (1976) 1675–1682.
[10] Denoël, V., Degée, H., 2005. Cas particulier d'étude analytique de l'élément à frottement, Internal report 2005-1, Department M&S, University of Liege.
[11] D. Karnopp, Computer simulation of stick-slip friction in mechanical dynamic systems, J. Dyn. Syst. Meas. Control 107 (1) (1985) 100–103.
[12] A.J. Morin, New friction experiments carried out at metz in 1831–1833, Proc. Fr. R. Acad. Sci. 4 (1833) 1–128.
[13] H. Olsson, K.J. Aström, C. Canudas de Wit, M. Gäfvert, P. Lischinsky, Friction models and friction compensation, Eur. J. Control 4 (12) (1998) 176–195.
[14] E. Rabinowicz, The nature of the static and kinetic coefficients of friction, J. Appl. Phys. 22 (11) (1951) 1373–1379.